RSC Advances

PAPER

View Article Online
View Journal | View Issue

Cite this: *RSC Adv.*, 2014, **4**, 29157

Phenylalanine-containing self-assembling peptide nanofibrous hydrogel for the controlled release of 5-fluorouracil and leucovorin†

N. Ashwanikumar,[a] Nisha Asok Kumar,[b] S. Asha Nair[b] and G. S. Vinod Kumar*[a]

Received 11th May 2014
Accepted 10th June 2014

DOI: 10.1039/c4ra04393f

www.rsc.org/advances

In the present study, we report a phenylalanine (Phe)-containing self-assembling peptide nanofibrous material (RATEA-F8) for the delivery of the drug 5-fluorouracil (5-FU) and leucovorin (LV), which exhibit synergistic actions against colon cancer. Solid phase peptide synthesis, followed by morphological characterisation of the material, depicts a facile formation of nanofiber in a time-dependent manner. Structural analysis and physical characterisation of the material were performed by transmission electron microscopy (TEM), circular dichriosm, spectrofluorimetry and oscillatory rheology. The *in vitro* release was also studied for 5-FU, LV and a model molecule namely Phe. The facile cellular uptake (monitored using confocal microscopy) and significant amount of cytotoxicity displayed by the drug entrapped peptide nano material further confirms the efficacy of the developed system for the drug delivery purpose.

Introduction

The autonomous organisation of materials into distinct hierarchical architectures, at microscopic and macroscopic levels, can be termed as self assembly. This process plays a major role in designing nanostructures and fine tuning their properties.[1] Non-covalent interactions govern the process of self assembly to a considerable extent. The predominant non-covalent forces include ionic, hydrogen, van der Waal's, hydrophobic, coordination bonds, and aromatic π–π stacking.[2–4] A tailored design of nanomaterials provides a platform to manipulate these interactions in order to get the desired properties of the materials.

Peptide motifs provide versatile building blocks for the process of self-assembly with well-defined structures in a bottom-up approach.[5,6] Such self-assembling peptides (SAP)-based nanomaterials were extensively utilised for various biomedical applications such as tissue engineering,[7] wound healing,[8] *in vivo* bone regeneration,[9] drug delivery[10] *etc.* The fascination of researchers for peptide-based drug delivery systems is due to its advantages like biocompatibility and biodegradability. A distinct self-assembly pattern can be fine tuned by altering amino acid sequences and the conjugation of different chemical functionalities. Thus, the material can be adapted to a variety of architectures like vesicles, micelles, fibres, tubes, hydrogels, monolayer and bilayers.[11–13] Short self-assembling peptides can be easily synthesised by standard solid phase protocols, with potential benefits like high purity, good yield, devoid of heterogeneity in molecular weight *etc.*

Amphiphilic peptides comprises alternating hydrophilic and hydrophobic amino acid sequences, governing the process of self-assembly through ionic interactions.[14] Alternating regular repeats of positively and negatively charged amino acids imparts unique structural features to such oligopeptides. RATEA-16 is one of the examples of SAP, which forms a nanofibrous hydrogel with tunable properties, as reported earlier.[15] We modified its 8th position with phenylalanine (Phe) to gain the property of interpeptide aromatic π–π stacking, along with the existing non-covalent interactions. Phenylalanine proved to be an ideal choice, unlike other aromatic amino acids (tryptophan, tyrosine and histidine), as its neutral nature and structural geometry maintain the beta sheet geometry of RATEA-16. The introduction of aromatic groups into the peptide sequence will enhance the loading and release of guest molecules containing aromatic ring, due to aromatic π–π interactions.[16,17]

The use of SAP as drug delivery vectors has been successfully demonstrated with different molecules like ellipticine,[18] curcumin,[19] doxorubicin,[20] dexamethasone[21] *etc.* In the present paper, we have demonstrated the use of a new class of peptide RATEA-F8 for the delivery of 5-fluorouracil (5-FU) and leucovorin (LV). 5-FU and LV shows synergistic action against colon cancer,[22] and LV was found to increase the extent of thymidylate synthase inhibition (5-FU-Potent thymidylate synthase inhibitor), resulting in the depletion of cellular thymidine leading to apoptosis.[23] To enhance the efficacy of 5-FU, the drug needs to be administered using suitable drug delivery systems (DDS).[24]

[a]*Chemical Biology, Rajiv Gandhi Centre for Biotechnology, Poojappura, Thiruvananthapuram-695 014, Kerala, India. E-mail: gsvinod@rgcb.res; Fax: +91-471-2348096; Tel: +91-471-2529526*

[b]*Cancer Research Programme, Rajiv Gandhi Centre for Biotechnology, Poojappura, Thiruvananthapuram-695 014, Kerala, India*

† Electronic supplementary information (ESI) available. See DOI: 10.1039/c4ra04393f

Facile solid phase synthesis of RATEA-F8, analysis of structure, morphology and gelation behaviour, *in vitro* release studies, cellular uptake studies and cytotoxicity assay in colon cancer cell line are the key points substantiating the fact that RATEA-F8 can be used as an efficient vector for the delivery of 5-FU and LV. The RATEA-F8 hydrogel can be administered orally through pH-sensitive polymer-coated capsules.[25]

Experimental section

Materials

Fmoc-protected amino acids like Fmoc-Ala.H_2O, Fmoc-Arg(Pbf) Fmoc-Glu(OBu^t), Fmoc Thr(OtBu) and Fmoc-Phe and TentaGel™ –S–NH_2 were purchased from Peptide international Inc. Fmoc Rink linker was purchased from Novabiochem. Trizma base, 8-anilinonaphthalene-1-sulfonic acid ammonium salt (ANS); oupling reagents, hydrobenzoxy triazole (HOBT), diisopropylethylamine (DIEA), and *O*-benzotriazole-*N*,*N*,*N*′,*N*′-tetramethyl-uronium-hexafluoro-phosphate (HBTU); cleavage reagents, trifluoroacetic acid (TFA), triisopropylsilane (TIS) and Ninhydrin; Fluorotag® fluorescein isothiocyanate (FITC) conjugation kit; Fluoromount®; 5-fluorouracil (5-FU); 3-(4,5-dimethylthiazol-2-yl)-2,5-diphenyltetrazolium bromide (MTT); and β-actin were obtained from Sigma-Aldrich. Piperidine, dichloromethane (DCM), diethylether, *N*,*N*-dimethylformamide (DMF), and ethanol were obtained from Merck. Foetal bovine serum (FBS) was purchased from Gibco (Life Technologies AG, Basel, Switzerland). Cell Mask™ (plasma membrane staining kit) and RPMI-1640 were obtained from Invitrogen (Carlsbad, CA).

Synthesis of peptide

The CH_3-CO-RATARAEFRATARAEA-CO-NH_2 (RATEA-F8) peptide was synthesized using the Standard Fmoc-Strategy. TentaGel™–S–NH_2 resin was utilized, which was linked to Fmoc Rink linkers by standard HBTU/HOBt activation, and peptide synthesis was carried out using the standard Fmoc methods. After completion of the chain assembly, the peptide fragment was acetylated with acetic anhydride in DCM. Then, the peptide was manually cleaved using trifluoroacetic acid (TFA), triisopropylsilane (TIS), and water (95 : 2.5 : 2.5). (Synthetic scheme provided in the ESI†). Further, the peptide was precipitated with diethyl ether, followed by 10–15 washes with diethyl ether. After the purification, the peptide was dissolved in a minimum amount of water, lyophilised and stored at −20 °C. HPLC purification of the cleaved peptides was performed with a Shimadzu LC-AD HPLC system, equipped with a variable wavelength absorbance detector and a reverse phase C18 column. A binary gradient of water (0.1% TFA) and acetonitrile (0.1% TFA) at 1 mL min^{-1} was used, and the column eluents were monitored by UV absorbance at 215 and 254 nm. Fractions were collected and lyophilized after their purity was confirmed by analytical HPLC using an RP-C18 column. Peptide identity was verified by matrix-assisted laser desorption ionization mass spectroscopy (MALDI-TOF MS).

Preparation of hydrogel

The RATEA-F8 peptide (0.78% wt/v) was dissolved in Milli Q water and Tris–HCl buffer (pH 7.4). The hydrogel was gradually formed over time. The loading of different guest molecules (5-FU, LV and Phe) was achieved with the appropriate ratio (peptide–guest; 20 : 1). For *in vitro* cytotoxicity experiments, different concentrations of 5-FU and LV loaded in RATEA-F8 were prepared from the stock solution of 5-FU (5 mg mL^{-1} of Tris–HCl buffer, pH = 7.4) in a serial dilution manner.

Determination of entrapment efficiency

A known amount of the guest molecule-loaded RATEA-F8 was dissolved in H_2O–MeCN–TFA (7 : 2.8 : 0.2) to obtain a clear solution. The dissolved peptide was separated by precipitation with diethyl ether. Absorbance measurements of the aqueous layer were carried out at the corresponding wavelengths (5-FU = 266 nm, LV = 282 nm, Phe = 254 nm) using a LAMBDA 25 UV-vis spectrophotometer (PerkinElmer, Waltham, MA). The entrapped amount was calculated with the respective ratio between the actual entrapment ratio (AER) and the theoretical entrapment ratio (TER), expressed in terms of the amount of molecule per weight of hydrogel. The entrapment efficiency was determined by the following equation: entrapment efficiency (%) = AER/TER × 100 [AER = measured amount of guest molecule/measured peptide amount, TER = initial amount of guest molecule/initial peptide amount].

TEM analysis

The stepwise process of hydrogel formation was monitored by TEM analysis (TEM, JEOL 1011, and Japan). The peptide hydrogel (0.78% w/v) dissolved in Milli-Q® (Millipore Corporation, Billerica, MA) water was dropped on a copper-coated formvar microscopy grid at different time intervals (5, 10, 15, 20, 30 and 60 min). The grid was washed with 1 μL Milli-Q water and dried. TEM pictures were taken using Digital Micrograph and Soft Imaging Viewer software.

Fluorescence spectroscopy

Fluorescence studies were conducted using a FP-777 spectrofluorometer (JASCO). Experiments were performed at ambient temperature using a quartz cell with a 10 mm path length. In this study, ANS was used to measure amphiphilicity inside the peptide fibres.[26] The emission spectra of ANS (20 μM) were recorded for different concentrations of RATEA-F8 aqueous solutions (100 μM, 200 μM) excited at λ_{ex} = 356 nm.

Oscillatory rheology

Rheological measurements of RATEA-F8 were carried out at 37 °C using an Anton Paar Physica MCR 150 rheometer having a 20 mm stainless steel parallel plate. Samples were prepared as described earlier. Dynamic time sweep experiments were carried out to study the change in storage modulus (G') and loss modulus (G'') as a function of time (6 rad per s frequency, 0.2% strain) during 20 min.

CD measurement

Circular dichroism (CD) spectra were obtained using a JASCO J-820K spectropolarimeter, which was flushed with nitrogen during the operation. Wavelength scans were recorded at 0.1 nm intervals from 260 to 190 nm, using a 0.1 cm path length quartz cuvette. The spectra obtained were averaged from 16 consecutive scans and subtracted from the background. The measurements was expressed as mean residue ellipticity ([θ], deg cm^2 $dmol^{-1}$).

In vitro drug release studies

The *in vitro* release kinetics study of the loaded guest molecules were conducted to study the release behaviour and stability of the peptide hydrogel under physiological conditions. Freshly prepared phosphate buffered saline (PBS) at physiological pH was used in the experiment. The guest-loaded peptide hydrogel was placed inside a dialysis membrane (Mw CO 500 kDa) and subjected to shaking at 50 rpm in rotary shaker at 37 °C. In addition, 1 mL of the reaction mixture was withdrawn at different time intervals. The release profile was monitored over 900 min as an approximation of the gastrointestinal retention time.[27] Gastrointestinal retention time plays a major role because DDS deliver antineoplastic agents in the colon. The amount of guest molecules released was estimated using a UV-Visible Spectrophotometer (Perkin-Elmer, Lambda 25) at specific wavelengths (5-FU = 266 nm, Phe = 254 nm, LV = 282 nm).

Cell culture

HCT 116 cells were purchased from American Type Culture Collection (Manassas, VA) and maintained in RPMI supplemented with 10% FBS at 37 °C under humidified atmosphere containing 5% carbon dioxide. Once they reached 70% confluence in tissue culture flasks, the cells were trypsinized with phosphate buffered saline solution containing 0.25% trypsin and 0.03% EDTA.

Cell uptake studies

For cellular uptake studies, fluorescein isothiocyanate (FITC)-tagged RATEA-F8 peptides were prepared as follows. The peptides and FITC were dissolved in carbonate–bicarbonate buffer separately. After mixing, the solution was covered with foil and shaken overnight at 10–14 °C at 250 rpm in a Thermomixer (Eppendorff). Furthermore, the FITC conjugate was separated from free peptides on a G-25 column. FITC conjugates to the $-NH_2$ group of the peptide in the –N=C=S region through a thiourea bond. The *F*/*P* ratio, determined by spectrophotometry, showed a conjugation of 82.7% of RATEA-F8 with FITC. The conjugate was stabilized with 1% bovine serum albumin and 0.1% sodium azide, and stored at 0–5 °C for cellular uptake studies.

To study cellular uptake, HCT 116 colon cancer cells were cultured in a 12-well plate containing a sterile glass cover slip in complete growth media at a density of 8×10^3 cells for 24 hours. FITC-tagged RATEA-F8 was then added to the culture media at a concentration of 200 μM. After 1 hour and 45 minutes of incubation at 37 °C, the cells were counterstained with Hoechst for 15 minutes. After PBS washing, the plasma membranes were stained with 1 μm of Cell Mask™ (Invitrogen, Carlsbad, CA) for 2–4 minutes. Then, they were washed twice with PBS and fixed with 4% paraformaldehyde for 30 minutes at room temperature. The cells were again washed twice with PBS and mounted using Fluoromount®. Moreover, the slides were analyzed under a confocal laser scanning microscope (CLSM) (Nikon Eclipse Ti (AIR), Japan) at wavelengths of 405 nm, 488 nm and 640 nm to view the blue, green and red fluorescence, respectively. The images were captured at a magnification of 63 × and scan speed of 400 Hz.

Cytotoxicity assay

MTT reduction assay was performed to assess the synergistic action of 5-FU and LV in naïve and nanoformulations to induce cytotoxicity. Briefly, cells were seeded (7×10^4 cells per well) in a 96-well culture plate and incubated for 24 hours. Cells were treated with formulations of 5-FU (1–100 μM) along with LV (0.1–10 μM) in nano and naïve form for 24, 48, and 72 hours. The ratio of 5-FU–LV was kept as 10 : 1 as previously described.[23,28] After the required duration of treatment, the media was aspirated, and 100 μL fresh media was added to the wells. Then, 10 μL (10% v/v) MTT (5 mg mL^{-1} in PBS) was added to each well, and the plates were further incubated at 37 °C for 4 hours. The assay determines cell viability based on the ability of mitochondrial dehydrogenase enzymes of the metabolically active cells to convert the water-soluble yellow MTT into water-insoluble purple formazan crystals. After 4 hours of incubation, the medium was completely removed, and the formazan crystals were dissolved in 100 μL isopropyl alcohol. The intensity of the colour yield is proportional to the number of metabolically active cells. The optical density was measured at 570 nm. The percentage of cell inhibition was calculated by the formula: [absorbance of control − absorbance of test]/[absorbance of control] × 100. Control cells are those cells treated with media alone.

Statistics

All the measurements were performed in triplicate, and the results were expressed as arithmetic mean ± standard error of the mean.

Results and discussion

Synthesis and characterisation of peptide hydrogel

The peptide RATEA-F8 was synthesised with a good yield and high purity by solid phase peptide synthesis technique. The molecular weight of peptide RATEA-F8 (Fig. 1A), determined by MALDI TOF MS, illustrates a value of 1789.146 which agrees with a calculated value (1789.9). This figure also shows the absence of other peaks, which indicates the absence of the addition or deletion of amino acids during synthesis. The purity of the peptide is demonstrated in the RP-HPLC profile by a single sharp peak, with a retention time of 4.657 min (Fig. 1B). The structural characterisation of the material is given in ESI.† The process of hydrogel formation was detected at the pH of

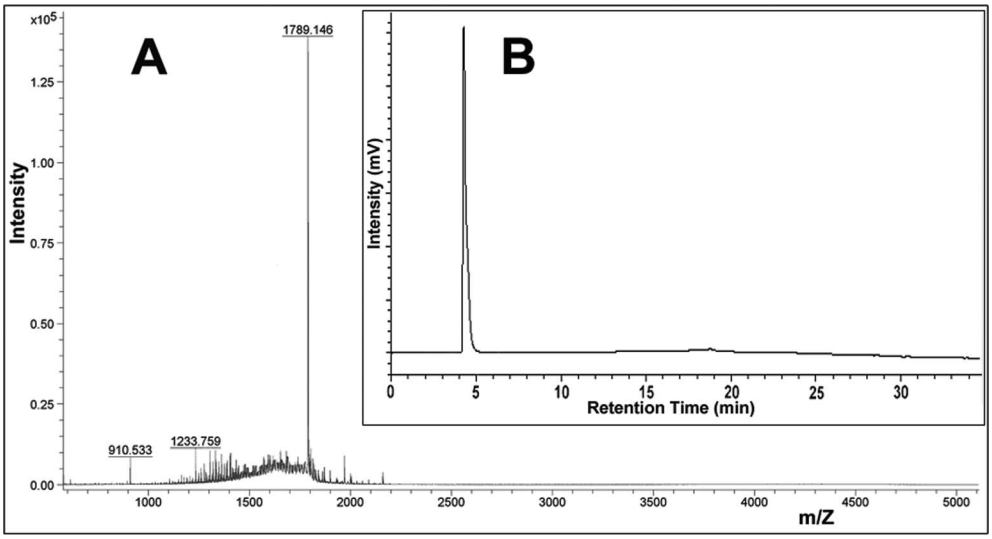

Fig. 1 (A) MALDI-TOF showing the mass of RATEA-F8 as 1789.146. (B) RP-HPLC profile of RATEA-F8.

Table 1 Entrapment efficiency of the loaded guest molecules[a]

Guest molecules loaded in RATEA-F8	Entrapment efficiency (%)
5-FU	82.4 ± 0.5
LV	74.7 ± 1.2
Phenylalanine	93.5 ± 0.8

[a] Data represents mean ± standard deviation (SD) ($n = 3$).

7.4. Hydrogel formation was independent of the loaded molecules such as 5-FU, LV and phenylalanine.

The loaded guest molecules exhibited good entrapment efficiency with the peptide (Table 1). The extent of loading was found to be dependent on the structure of the guest molecules. The variation in encapsulation may be attributed to the size and aromaticity of the molecule.[29] Phe was selected as a model molecule since it is assumed to form a good amount of aromatic π–π stacking with the Phe of the RATEA-F8 peptide. In accordance with our hypothesis, Phe displayed significantly high value of guest molecule loading (Table 1). LV showed slightly lower value due to steric hindrance, whereas 5-FU provided a fairly higher amount of loading than LV due to its small structure, although the aromaticity of 5-FU is lower than that of LV.

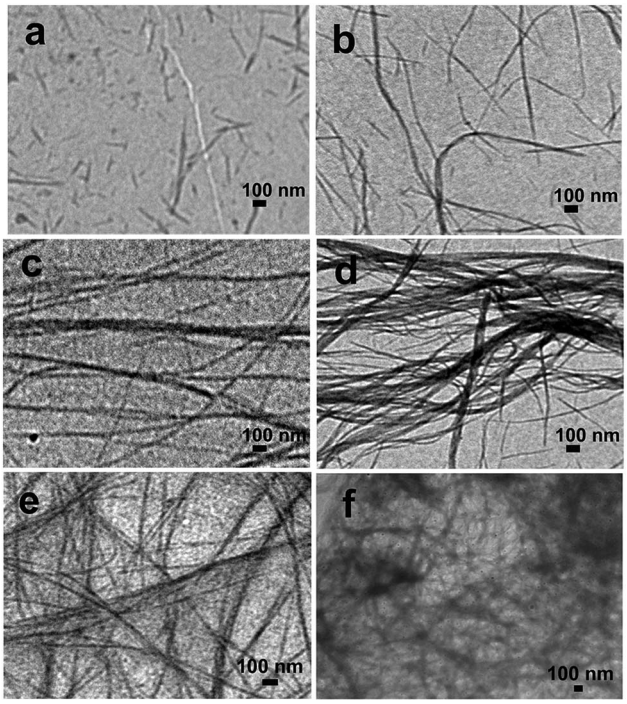

Fig. 2 Transmission electron microscopy (TEM) images of nanofiber formation (a) after 5 min, (b) after 10 min, (c) after 15 min, (d) after 20 min, (e) after 30 min, and (f) after 60 min.

Nanostructure of the peptide hydrogel

Transmission electron microscopy (TEM) aided us in the investigation of the slow process of hydrogel formation of RATEA-F8 peptide. Time-dependent analysis of the peptide hydrogel illustrated the process of nanofiber formation, as shown in Fig. 2a–f. In Fig. 2a, nanofiber formation was initiated with a diameter of 5–20 nm and a length of 60–80 nm. The individual peptides autonomously started to organise into a long tubular structure, which is more prominent in Fig. 2b. Further, in Fig. 2c and d, the length of the nanofibers begins to increase with the initiation of cross-linking. The important observation of cross-linking, with self-supporting hydrogel formation, was vividly observed after 30 min (Fig. 2e). The interconnecting nanofibres forms a highly dense cross-linked network after 1 hour, as observed in Fig. 2f. Thus, the supramolecular self-assembly of peptide nanofibers resulted in the formation of a self-supporting hydrogel.

The amphiphilicity of the peptide nanofibres were analysed by spectrofluorimetric analysis (Fig. 3a). The ANS probe binds to the specific hydrophobic regions of the peptide nanofibres,

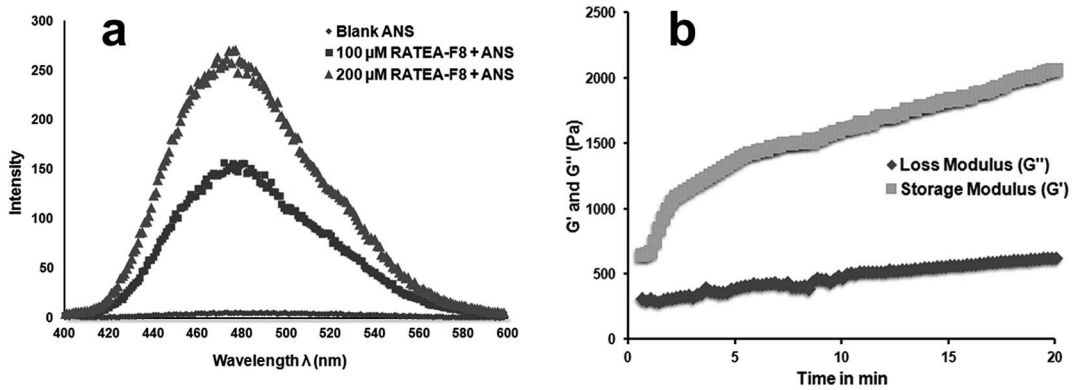

Fig. 3 (a) Spectrofluorimetric analysis of SAPNS of RATEA-F8 at two different concentrations (100 μM and 200 μM) using an ANS probe. (b) Rheological analysis of RATEA-F8 by dynamic time-sweep experiment to monitor the variations in storage modulus (G') and loss modulus (G'') over 20 min.

emitting at 475 nm. In comparison with the blank ANS, the peptide solution with ANS demonstrates a blue shift in intensity in concentration-dependent manner. These observations suggest that an ordered supramolecular self-assembly of the peptide nanofibres arises due to the amphiphilic nature of the peptide, as Ala and Phe contribute to the hydrophobicity, whereas Arg, Glu and Thr impart hydrophilicity to the peptide.[17] Rheological analysis of the material displays the gel-like behaviour of the material. The dynamic time sweep (DTS) experiment carried out confirms the above fact. During the experimental time period, the storage modulus (G') remains more than the loss modulus (G''), which depicts the gel nature of the peptide material (Fig. 3b).

To gain insights into the structural organisation of the peptide nanofibres, CD measurements were carried out (Fig. 4). These data substantiate the antiparallel beta-sheet structure of the material. The spectra show two distinguishable peaks at 197 nm and 216 nm, which are of antiparallel beta-sheet arrangement (Fig. 4a). This is in agreement with the structure of RATEA-16 reported earlier, indicating that our modification with Phe does not alter the secondary structure of the material.[15] The structural organisation of the peptides were found to be disruptive at a very high basic pH of 12.5, whereas it was quite stable at pH 3 and pH 7.4. This observation substantiates the use of the peptide for drug delivery applications at physiological pH, especially in the colon. Further, the entrapment of molecules like 5-FU and LV was not found to influence the formation of the beta-sheet geometry of the peptide. The inherent secondary structure was retained, irrespective of either peptide primary sequence modification or guest molecules (5-FU, LV, Phe) loading as witnessed in CD spectral analysis (Fig. 4b) .The above observations like pH-dependent stability and nature of the peptide after molecular entrapment makes it highly useful for drug delivery applications.

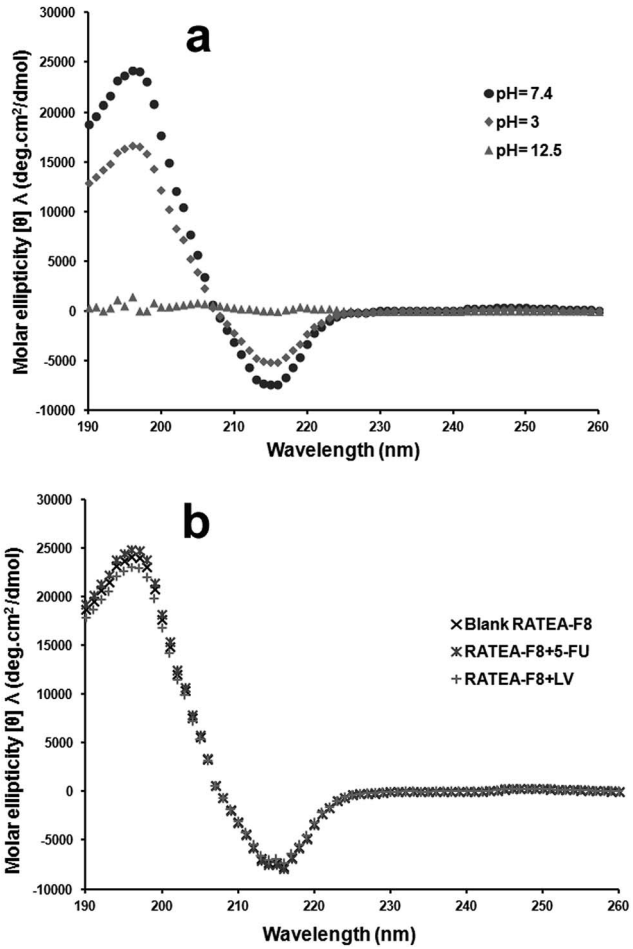

Fig. 4 CD spectra of RATEA-F8 under different conditions. (a) Blank RATEA-F8 at three different pH (pH 3, pH 7.4 and pH 12.5). (b) Comparison of the CD patterns of RATEA-F8 with and without guest molecules.

Effective loading of guest molecules inside the peptide nanofibrous scaffold

In situ preparations of peptide hydrogel and loading of guest molecules were successfully achieved. Good encapsulation efficiency was observed for all the loaded molecules. The inherent antiparallel beta-sheet arrangement was ascertained by the CD spectra and the formation of a hydrophobic core was detected by fluorescence measurements in the presence of ANS.

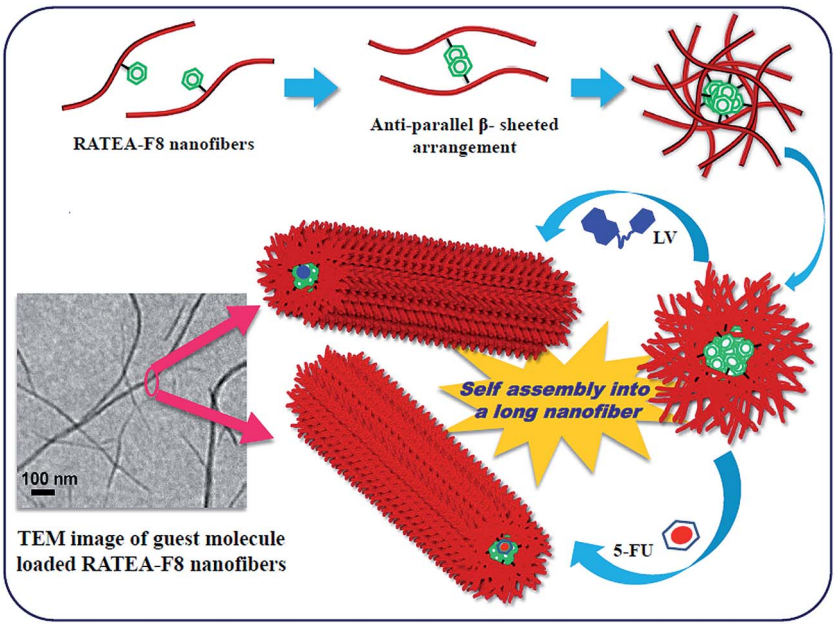

Fig. 5 Schematic representation of the stepwise hierarchical self-assembly of peptide nanofibers, followed by guest molecule entrapment.

Based on the above observations, we propose a plausible mechanism for the loading of guest molecules inside the peptide nanofibres, as shown in Fig. 5. The molecules were effectively placed inside the aromatic core of the peptide nanofibres of tubular shape. The individual nanofibers further elongate and interconnect with each other to form a self-supporting hydrogel.

The controlled release of the guest molecules was monitored using *in vitro* release kinetics experiment (Fig. 6). All the three molecules show a kind of burst release mechanism during the initial 60 minutes. However, later they follow the Peppas model release from the scaffold.[30] Phe shows a more controlled and prolonged release from the nanofibres. The burst release was prominent in case of LV compared to that of the other two molecules, which may be due to the large size of the molecule. (See ESI.†) After 400 minutes, all the loaded guest molecules reached almost a steady state. Afterwards, only a small amount of increment in release was observed upto 900 min.

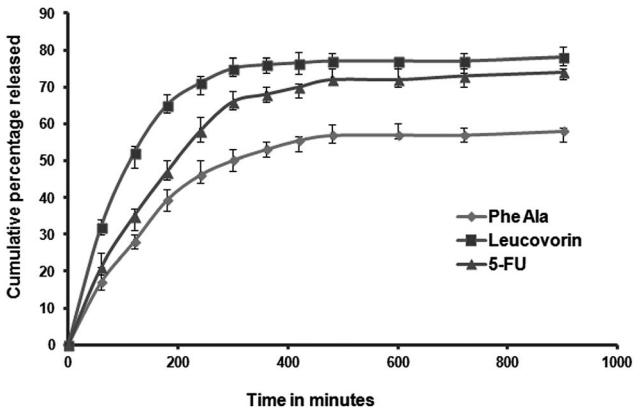

Fig. 6 *In vitro* release profile of guest molecules from RATEA-F8.

Uptake of the peptide nanofibres into colon cancer cell line

The cellular internalisation of the nanofibres was visualised with CLSM by FITC-tagged peptides. The nanofibres were readily internalised as early as 2 hours of incubation (Fig. 7). The CLSM images clearly depict the localisation of green colour in the cytoplasmic region of HCT 116 cells *in vitro*.

The counterstaining with red and blue dyes allowed us to track the location of the nanofibres more clearly and precisely. The cellular uptake results firmly support the use of RATEA-F8 nanofibrous material as DDS to cancer cells.

Significant cytotoxicity of the peptide nanofibres along with synergistic activity of 5-FU and LV

The nanofibres demonstrated a considerable amount of cytotoxicity when entrapped with 5-FU and LV (Fig. 8). The cell viability assay shows the synergistic activity of the two molecules 5-FU and LV. The synergism was analysed at 5 FU to LV ratio 10 : 1 at 24, 48 and 72 hours. In Fig. 8, the concentration indicates the 5-FU concentration in μM level (each concentration of 5-FU + LV consists of 5-FU and LV in a 10 : 1 manner). After 24 hours, the synergistic activity was evident for 5, 10, 50, 75, 100 μM concentration, whereas in nanoformulation, the activity was found to be significantly higher for the concentration of 1, 5, 10, 50 and 100 μM.

The activity of the nanoformulation of 5-FU and LV was found to increase to appreciable level for all the experimental concentration after 48 and 72 hours, which is a vital observation in terms of an ideal drug delivery system. The synergistic activity was also found for 5, 10, 25, 50 and 100 μM after 48 hours and 1, 5, 10, 25, 75 and 100 μM after 72 hours. The biocompatibility of RATEA-F8 was vividly depicted in all the experimental time periods as the cell viability was observed for all the concentration. Therefore, we can confirm the decisive action of the

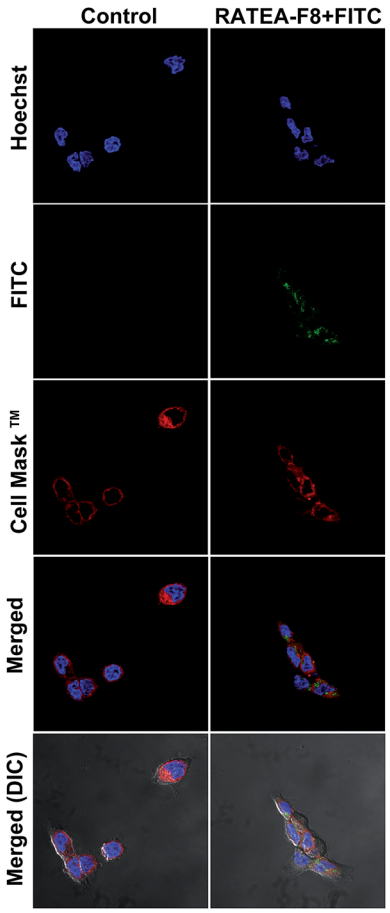

Fig. 7 Cellular uptake of FITC-tagged RATEA-F8 by HCT-116 cells after 2 h of incubation. DIC, differential interference contrast; FITC, fluorescence isothiocyanate; Cell Mask™, plasma membrane dye for Hoechst-nuclear staining.

nanoformulation (5-FU- and LV-entrapped RATEA-F8) along with synergism. IC_{50} values of the samples were calculated from the dose response curve, and the values are given in Table 2.

After 48 hours, IC_{50} value for the nanoformulation was 3 times lower than that for the naïve drug combination. The value became exceptionally significant (~15 times lower) after 72 hours of incubation. These observations confirm the potency of RATEA-F8 nanofibres for the delivery of small aromatic molecules with high efficacy.

The biological evaluation evidently depicted the felicitous use of RATEA-F8 for the controlled release of drugs from nanoformulations at high efficacy. Although different DDS with the delivery of synergistic agents have been reported earlier, we present RATEA-F8 as the first peptide-based system for the sustained release of 5-FU and LV. The nanofibres were readily internalised by the HCT-116 cells within 3 hours of incubation due to their small size. Furthermore, cytotoxicity measurements demonstrated the induction of cancer cell death at a low dose, with significant IC_{50} values. Thus, the combined physical and biological assessment of the peptide nanofibres proves the efficacy of the DDS in colon cancer chemotherapy.

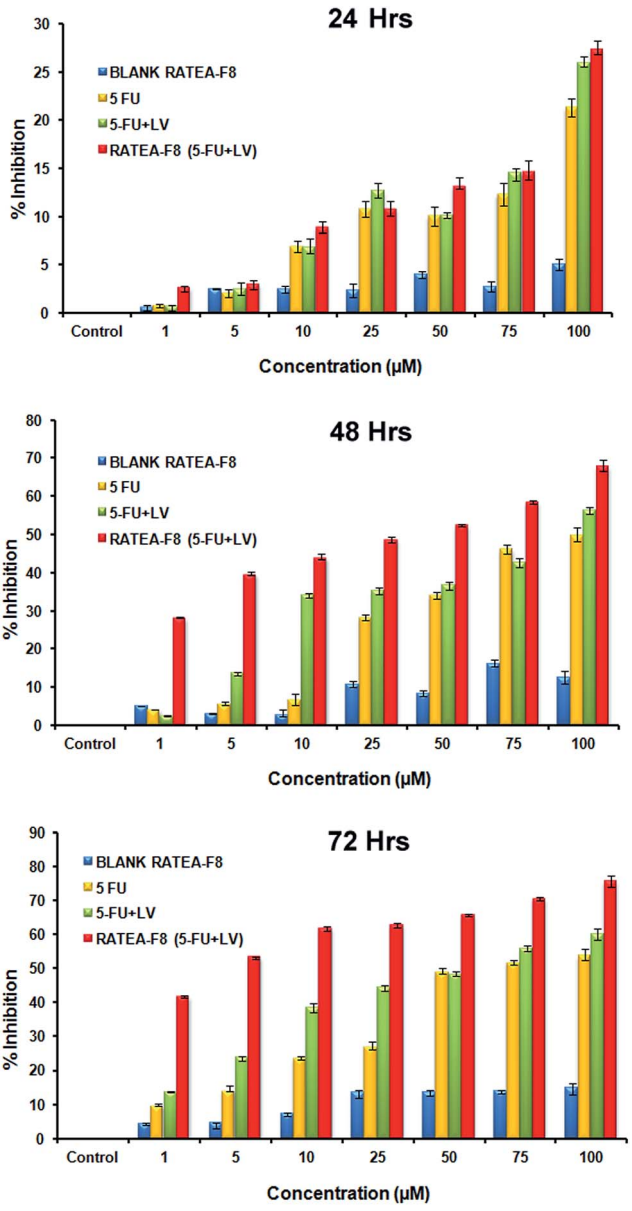

Fig. 8 MTT assay of 5-FU-loaded RATEA-F8 after 24 h, 48 h and 72 h. The data represents mean ± SD ($n = 3$).

Table 2 IC_{50} values of drug-entrapped RATEA-F8[a]

	IC_{50} values in μM		
Incubation time (hours)	5-FU	5-FU + LV	RATEA-F8 (5-FU + LV)
48	99.89	91.43	36.35
72	66.59	58.56	4.03

[a] Data represents mean ± standard deviation (SD) ($n = 3$).

Conclusion

Amino acids and peptides impart nanoarchitecture "smartness" to the supramolecular self-assembled materials. The bottom-up

design of such smart biomaterials opens up new avenues in drug delivery with desirable properties. Biocompatibility, benign processing at physiological conditions, and amphiphilicity are some of the key points, which support peptide-based DDS as potential candidates.[11,19] The bulk physical behaviour, such as the network stiffness, porosity, and ease of drug loading, can be adjusted by the peptide sequence. The present work depicts such an apt peptide-based DDS for the anticancer drug delivery application. Here, we have shown the convenient synthesis, characterisation, and *in vitro* evaluation of peptide nanofibres for the combined delivery of two molecules, namely 5-FU and LV. The process of self-assembly, encapsulation, and cytotoxicity were achieved in a felicitous manner. The coherent results, shown by the physicochemical and biological assessment of the material, puts forward an innovative approach in DDS. Although more biological studies and *in vivo* study models are essential, the present study provides a strong platform for the co-delivery of antineoplastic agents.

Acknowledgements

The authors are thankful to Ms Rintu Varghese and Mr Anuroop K. G. of the Rajiv Gandhi Centre for Biotechnology (RGCB) for the TEM and CLSM analyses, respectively, Dr Sudha J. D. of the National Institute for Interdisciplinary Science and Technology (NIIST) Trivandrum for the rheological analysis, the Indian Institute of Science Education and Research (IISER) Trivandrum for the CD analysis, the Department of Biotechnology, New Delhi for providing the financial assistance for the research, and the Council for Scientific and Industrial Research (CSIR), New Delhi for the Junior Research Fellowship to N. Ashwanikumar.

Notes and references

1 E. Busseron, Y. Ruff, E. Moulin and N. Giuseppone, *Nanoscale.*, 2013, **5**, 7098–7140.
2 R. V. Ulijn and A. M. Smith, *Chem. Soc. Rev.*, 2008, **37**, 664–675.
3 R. J. Mart, R. D. Osborne, M. M. Stevens and R. V. Ulijn, *Soft Matter*, 2006, **2**, 822–835.
4 K. Rajagopal and J. P. Schneider, *Curr. Opin. Struct. Biol.*, 2004, **14**, 480–486.
5 X. Yan, P. Zhu and J. Li, *Chem. Soc. Rev.*, 2010, **39**, 1877–1890.
6 T. Koga, H. Matsui, T. Matsumoto and N. Higashi, *J. Colloid Interface Sci.*, 2011, **358**, 81–85.
7 L. Zhang and T. J. Webster, *Nano Today*, 2009, **4**, 66–80.
8 R. G. Ellis-Behnke, Y.-X. Liang, S. W. You, D. K. Tay, S. Zhang, K. F. So and G. E. Schneider, *Proc. Natl. Acad. Sci. U. S. A.*, 2006, **103**, 5054–5059.
9 H. Hosseinkhani, M. Hosseinkhani, F. Tian, H. Kobayashi and Y. Tabata, *Tissue Eng.*, 2007, **13**, 11–19.
10 X. D. Xu, L. Liang, C. S. Chen, B. Lu, N. l. Wang, F. G. Jiang, X. Z. Zhang and R. X. Zhuo, *ACS Appl. Mater. Interfaces*, 2010, **2**, 2663–2671.
11 Y. Loo, S. Zhang and C. A. Hauser, *Biotechnol. Adv.*, 2012, **30**, 593–603.
12 S. S. Babu, V. K. Praveen and A. Ajayaghosh, *Chem. Rev.*, 2014, **114**, 1973–2129.
13 Y. Nagai, L. D. Unsworth, S. Koutsopoulos and S. Zhang, *J. Controlled Release*, 2006, **115**, 18–25.
14 X. Zhao and S. Zhang, *Chem. Soc. Rev.*, 2006, **35**, 1105–1110.
15 Y. Zhao, H. Yokoi, M. Tanaka, T. Kinoshita and T. Tan, *Biomacromolecules*, 2008, **9**, 1511–1518.
16 M. Reches and E. Gazit, *Nat. Nanotech.*, 2006, **1**, 195–200.
17 Y. Zhao, M. Tanaka, T. Kinoshita, M. Higuchi and T. Tan, *J. Controlled Release*, 2010, **142**, 354–360.
18 S. Y. Fung, H. Yang, P. T. Bhola, P. Sadatmousavi, E. Muzar, M. Liu and P. Chen, *Adv. Funct. Mater.*, 2009, **19**, 74–83.
19 A. Altunbas, S. J. Lee, S. A. Rajasekaran, J. P. Schneider and D. J. Pochan, *Biomaterials*, 2011, **32**, 5906–5914.
20 S. Zarzhitsky and H. Rapaport, *J. Colloid Interface Sci.*, 2011, **360**, 525–531.
21 M. J. Webber, J. B. Matson, V. K. Tamboli and S. I. Stupp, *Biomaterials*, 2012, **33**, 6823–6832.
22 C. M. Tsai, S. H. Hsiao, C. M. Frey, K. T. Chang, R. P. Perng, A. F. Gazdar and B. S. Kramer, *Cancer Res.*, 1993, **53**, 1079–1084.
23 I. Petak, D. M. Tillman and J. A. Houghton, *Clin. Cancer Res.*, 2000, **6**, 4432–4441.
24 T. S. Anirudhan and A. M. Mohan, *RSC Adv.*, 2014, **4**, 12109–12118.
25 E. T. Cole, R. A. Scott, A. L. Connor, I. R. Wilding, H. U. Petereit, C. Schminke, T. Beckert and D. Cade, *Int. J. pharm.*, 2002, **231**, 83–95.
26 A. Accardo, D. Tesauro, L. Del Pozzo, G. Mangiapia, L. Paduano and G. Morelli, *J. Pept. Sci.*, 2008, **14**, 903–910.
27 L. Yang, J. S. Chu and J. A. Fix, *Int. J. Pharm.*, 2002, **235**, 1–15.
28 N. W. Wilkinson, G. Yothers, S. Lopa, J. P. Costantino, N. J. Petrelli and N. Wolmark, *Ann. Surg. Oncol.*, 2010, **17**, 959–966.
29 Y. Zhao, M. Tanaka, T. Kinoshita, M. Higuchi and T. Tan, *J. Controlled Release*, 2010, **147**, 392–399.
30 B. Kim, K. La Flamme and N. A. Peppas, *J. Appl. Polym. Sci.*, 2003, **89**, 1606–1613.

